A Simple Model of the Free Electron Laser Oscillator from Low into High Gain

B. W. J. McNEIL

Abstract—**This paper presents an investigation of the Compton free electron laser oscillator from the low into the high gain regime. The one-dimensional Maxwell–Pendulum equations, describing the radiation–electron beam evolution in an FEL, are used to develop a simple, computationally efficient method of modeling the radiation evolution. The maximum efficiency for a range of values of the gain parameter G is calculated.**

Introduction

FREE electron lasers (FEL's) operating in the Compton limit, where electron beam space-charge effects are negligible, have demonstrated their ability to provide tunable sources of high-power coherent radiation operating at wavelengths and power levels not accessible by other conventional laser systems [1].

Historically, these FEL's have been categorized into two distinct groups: high gain and low gain devices [1]. These categories may be distinguished by the FEL Gain Parameter, $G = 4\pi\rho N_w$; where N_w is the number of wiggler periods and ρ is the fundamental FEL or Pierce parameter [2], which is proportional to the cubic root of the electron beam density ($\propto n_e^{1/3}$) and is inversely proportional to the dimensionless beam energy ($\propto \gamma^{-1}$).

High gain is defined for $G > 1$, and low gain for $G < 1$, with a transition region around $G \simeq 1$. In high gain devices the electrons interact cooperatively via the potential wells (or "buckets") formed by the combined radiation–wiggler fields [3]. The electrons interact cooperatively by bunching in, and thereby changing the phase of these potential wells, thus resulting in an exponentially growing instability in the radiation field amplitude. This exponential growth ceases if the system saturates, i.e., when the electrons begin to perform synchrotron oscillations in the ponderomotive potential wells. The cooperative effect of the electrons is reflected in the scaling of the radiation intensity as $\propto n_e^{4/3}$ [2].

Such high gain FEL's can been used in a single-pass amplifier configuration, starting from an injected signal, or from noise to produce self amplified spontaneous emission (SASE). Whether or not the FEL reaches saturation (and therefore peak output intensity) depends upon the gain and the initial field amplitude at the beginning of the laser.

When $G < 1$, an FEL is in the low gain regime and the change in the radiation field is not sufficient to allow the electrons to interact cooperatively in one pass through the laser. A mismatch in the electron and ponderomotive well velocities (the detuning) is now required for an energy exchange between the electrons and the radiation [3]. For any appreciable output of radiation, the laser requires an oscillator cavity in which the radiation intensity can build up until the gain equals the cavity losses. As the radiation intensity increases in the cavity, electrons can become trapped within the ponderomotive wells. These electrons will then begin to execute synchrotron oscillations and the gain mechanism saturates [1].

Recent progress in accelerator technology, in particular the development of the photocathode [4], now means that significantly higher currents are available from some accelerators. These higher currents may take existing (Los Alamos, NM, RF linac. [5], [6]), and proposed (University of Twente, race-track microtron [7]), FEL oscillator experiments from the low gain–high gain transition region ($G \simeq 1$) into the high gain regime proper ($G > 2$), creating the high gain FEL oscillator.

As well as these experiments in the infrared region of the spectrum, this high gain regime of the FEL oscillator is also of interest in FEL designs for the ultraviolet and higher frequencies. The lack of high mirror reflectivities for these frequencies severely restricts the design of low gain oscillators.

This paper presents an investigation of the high gain oscillator regime, using the one-dimensional Maxwell–Pendulum equations in the steady-state (continuous electron beam) limit. These equations are solved for a range of input radiation intensities to construct tables of input versus output intensities for the desired values of G. These tables can then be used to follow the evolution of the radiation intensity in a FEL oscillator from the low to the high gain regimes.

A simple plane mirror cavity is assumed with zero diffraction of radiation, all losses being due to the output mirror transmission. Only the case of an untapered wiggler is considered and a wide range of values of G, from low to high gain, is investigated. Optimization of the electron beam detuning parameter and output mirror reflectivities is performed to find the maximum efficiency for a range of G.

Manuscript received July 28, 1989; revised October 29, 1989. This work was supported by the Dutch Foundation for Fundamental Research on Matter (FOM).

The author is with the Netherland's Center for Laser Research, University of Twente, Enschede, 7500 AE, The Netherlands.

IEEE Log Number 9035213.

The One-Dimensional Maxwell–Pendulum Equations

All results and simulations presented below follow from solutions to the 1-D Maxwell–Pendulum (M-P) equations familiar to Compton FEL theory (see [2], [8], [9] and references therein where the detailed derivations and approximations used can be found). The main restrictions of the equations as used here are their limitations to the steady-state regime, i.e., no pulse effects are included so that a continuous electron beam is assumed. The M-P equations are written in terms of the "universal scaling" of [8]:

$$\frac{dA}{d\tau} = \langle \exp(-i\theta) \rangle \tag{1a}$$

$$\frac{d^2\theta_j}{d\tau^2} = -(A \exp(i\theta_j) + \text{c.c.}), \quad j = 1, \ldots, N_e \tag{1b}$$

where A is the scaled complex field amplitude $A = |A| \exp(i\phi)$; $|A|^2 = \epsilon_0 |E|^2 / \rho n_e \gamma_r mc^2$; E is the radiation electric field; N_e is the number of electrons used in the simulation; $\langle\ \rangle$ is an average over the electrons $1/N_e \sum_{j=1}^{N_e}$; $\theta_j + \phi = (k_r + k_w)z - \omega_r t + \phi$ is the phase of the jth electron relative to the ponderomotive potential; $\tau = 2\omega_w \rho t$ is the scaled time through the wiggler; γ_r is the resonant electron energy in units mc^2; n_e is the electron beam density; k_w and k_r are the wiggler and radiation wavenumbers, respectively; $\omega_r = ck_r$; $\omega_w = c\beta_z k_w$; β_z is the resonant axial electron velocity in units of c; $K = eB_w/mck_w$ is the wiggler deflection parameter; B_w is the wiggler peak magnetic field strength, and ρ is the fundamental FEL parameter given by

$$\rho = \left[\frac{K}{4\omega_w} \left(\frac{en_e}{\epsilon_0 m \gamma_r^3} \right)^{1/2} \right]^{2/3}. \tag{2}$$

(In deriving (1) an helical wiggler configuration is assumed, however the same set of equations can be used for a planar wiggler if the value of ρ is multiplied by $(\Gamma^2/2)^{1/3}$, where Γ is the usual Bessel function factor [10].)

It has been assumed here that on injection into the FEL the electron beam is monoenergetic at the resonant energy defined by $2\gamma_r^2 = k_r(1 + K^2)/k_w$. Variations from this resonant energy at $\tau = 0$ are included in the detuning parameter

$$\delta = d\theta(\tau = 0)/d\tau = (\gamma(\tau = 0) - \gamma_r)/\rho\gamma_r. \tag{3}$$

(We note that in [2] and [8] this parameter is included in the equations explicitly—the two sets of equations are however equivalent.)

These M-P equations describe the self-consistent evolution of the electrons–radiation in weak and strong fields for low and high gain steady-state Compton FEL's. The integration interval for one pass through the FEL is $0 < \tau < G(= 4\pi\rho N_w)$, where G is the FEL gain parameter. FEL's with $G > 1$ are considered high gain and $G < 1$, low gain.

From the definitions in (1), it is seen that the radiation intensity scales as

$$|E|^2 \propto \rho n_e \gamma_r A^2 \tag{4}$$

and the efficiency

$$\eta = \rho(A_G^2 - A_0^2) \tag{5}$$

where $A^2 = |A|^2$; $A_G = A(\tau = G)$; $A_0 = A(\tau = 0)$.

By linearizing (1), (see [2]) and using the method of Laplace transforms, the radiation evolution (and hence the gain) can be found in the small-signal limit as a function of the detuning δ.

In the low gain limit $G < 1$ the familiar asymmetric Madey curve is obtained for the gain as a function of the detuning, with maximum gain occurring for $G\delta \simeq 2.6$ [3]. In the high gain limit $G >> 1$, the exponential instability dominates and maximum gain occurs for $\delta \simeq 0$, [2]. In the intermediate region of $G \simeq 1$ however, neither the Madey nor the high gain effects can be said to dominate as is seen in Fig. 1 where the small-signal gain

$$\text{SSG} = \frac{(A_G^2 - A_0^2)}{A_0^2} \tag{6}$$

is plotted as a function of $G\delta$ for $G = 2.0$.

In the oscillator simulations that follow, we wish to inject the monoenergetic electron beam with the optimized detuning for maximum small-signal gain. This ensures that it is that oscillator mode with the largest growth rate which is initially amplified. Any evolution in the mode (frequency) being amplified would be seen as an evolution in the rate of change of the radiation phase ϕ. In Fig. 2, $G\delta_{\text{opt}}$ (where δ_{opt} is the value of δ for maximum small-signal gain) is plotted as a function of G. It is seen that for $G < 1$, $G\delta_{\text{opt}}$ is close to the Madey curve value of 2.6, whereas for $G > 1$, $G\delta_{\text{opt}}$ decreases to a minimum of $\simeq 1.55$ around $G \simeq 4.3$, and then tends to an approximate limit of $\simeq 1.6$ to 1.7 in the limit of large G.

It should be emphasized that Fig. 2 is only valid in the small signal–linear region of evolution of (1). Because of this, the values of δ_{opt} for $G >> 1$ will not, for realistic initial conditions, be strictly accurate as the electron–radiation evolution will have left the linear and entered the saturated regime. A more accurate value for δ_{opt} would be that value taken at $G = \tau_{\text{sat}}$, where τ_{sat} is the value of τ required to bring the system to saturation. From a numerical integration of (1) a typical value, for realistic input parameters ($A_0^2 = 10^{-6}$, $\delta = 0$), is $\tau_{\text{sat}} \simeq 10.5$. This gives $G = \tau_{\text{sat}}$ from Fig. 2, $\delta_{\text{opt}} \simeq 0.16$. With this value of δ_{opt} used in a further numerical integration of (1), the intensity has a faster growth rate and saturates at $A_0^2 \simeq 1.57$. This corresponds to an increase in the saturated intensity of $\simeq 12\%$ from that value of $\simeq 1.4$ quoted in previous publications [2], [8], [9] where it has been assumed that maximum growth rate (gain) is at $\delta = 0$.

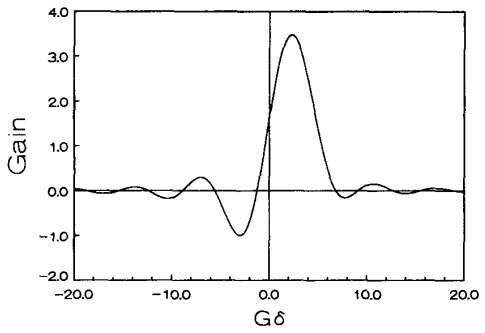

Fig. 1. Small-signal gain as function of $G\delta$ for $G = 2.0$.

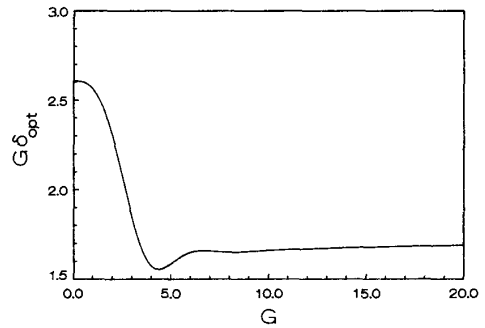

Fig. 2. $G\delta_{opt}$ as function of G.

The Oscillator Model

The results of the previous section are now used to set up a model of the FEL oscillator for both the low and high gain regimes.

The oscillator considered is that of a simple plane mirror cavity, with all radiation losses due to the transmission of the output coupling mirror of reflectivity R. It is assumed that the radiation wavelength produced by the FEL is sufficiently small compared to the cavity length as to allow the assumption of a quasi-continum of cavity normal modes at that wavelength, (this allows the variations in the phase of the radiation field between successive round-trips within the cavity to be neglected).

Equation (1) can be solved numerically for $A^{(n)}(\tau)$, (where the superscript refers to the number of round trips within the cavity), with initial conditions at the start of each round-trip of:

$$A_0^{(n)} = rA_G^{(n-1)} \tag{7}$$

where $r = \sqrt{R}$ and $A_0^{(1)} = A_0 \ll 1$. The assumption of a cavity normal mode continuum and the uniformly distributed electrons at the entrance to the wiggler in the range $0 < \theta_j^{(n)}(\tau = 0) < 2\pi$ allows an arbitrary radiation phase $\phi^{(n)}(\tau = 0)$, which is set to zero. The scaled output intensity

$$(A_{\text{out}}^{(n)})^2 = (1 - R)(A_G^{(n)})^2 \tag{8}$$

can then be calculated as a function of the number of cavity round trips n.

In order to investigate the effect of the output mirror reflectivity R on an FEL with predefined wiggler and electron beam parameters (i.e., a fixed value of G), a separate numerical simulation over many cavity round-trips for each value of R has to be performed using the above method. This requires large amounts of computer time. So when many simulations are to be executed, a more efficient method of modeling the output intensity was designed, and is now described.

For a given value of G, describing a particular wiggler–electron beam configuration, a table was constructed of A_G^2 versus A_0^2 for a single pass of the radiation–electrons through the laser. This was done by solving (1) (as a single-pass amplifier) for each value in the required range of A_0^2. 50 electrons were used with $\delta = \delta_{opt}$ and uniformly distributed in phase $0 < \theta_j(\tau = 0) < 2\pi$. By using the oscillator relation (7)

$$(A_0^{(n)})^2 = R(A_G^{(n-1)})^2 \tag{9}$$

with a given $(A_0^{(1)})^2$ and looking up the table (with linear interpolation) for each round-trip, a fast computational method of modeling the output intensity $(A_{\text{out}}^{(n)})^2$ is obtained. (Note that no information about the electron beam parameters are recovered directly from this model.)

This method of modeling the radiation intensity evolution in an FEL oscillator has proved to be accurate and reliable when compared with the full numerical integrations of (1). It does not tend to follow any small-scale detailed evolution but rather follows the general "averaged" evolution to acceptable accuracy. We now use the model to investigate the FEL oscillator in the high gain regime.

Results of the Oscillator Model

Before describing any results of the model, it is useful to describe an experiment in terms of the scaled parameters that are used here, and to demonstrate the effect on these parameters of the significant increase in current available to an FEL that a photocathode injector can provide.

The University of Twente, Enschede, The Netherlands, has a proposal to build an infrared FEL [7], based around a racetrack microtron accelerator. The parameters of the proposed FEL are electron energy $\simeq 25$ MeV (energy spread $\delta\gamma/\gamma \simeq 0.1\%$), $N_w \simeq 40$, $\lambda_w = 30$ mm, and $K \simeq 1$. For a current of $I \simeq 50$ A (such as may be provided by a thermonic electron gun) and an electron beam radius of $r_e \simeq 1.5$ mm, the value of parameters ρ and G are $\simeq 0.0028$ and $\simeq 1.4$, respectively. For an increase in the current available to approximately 400 A, as may be possible with the new photocathode injectors, the value of ρ doubles and so G increases to $\simeq 2.8$. As will be seen, this increase in the value of G takes the system out of the transition region between low and high gain regimes and just into the high gain regime proper. It is intended that the racetrack microtron will have a photocathode injector so that the FEL will actually operate as a high-gain oscillator device.

It is worth noting that the Los Alamos FEL [5], [6], has already been operational with a similar specification to that of the previous (for $I \simeq 40$ A) with $\rho \simeq 0.0025$ and $G \simeq 1.2$ and is shortly to have a new photocathode injector installed, possibly increasing the value of G to $\simeq 2.5$.

From tables of the type A_0^2 versus A_G^2 described in the previous section, we plot the increase in a single pass of the scaled intensity $A_G^2 - A_0^2$ as a function of A_0^2 in Fig. 3 for two values of the gain parameter (a) $G = 0.6$ (low gain), and (b) $G = 4.0$ (high gain). From this figure we can immediately make some general observations.

As we increase the value of A_0^2 (from $A_0^2 \ll 1$), $A_G^2 - A_0^2$ increases for both values of G (this is the small-signal linear regime). This continues until the values of A_0^2 become large enough to allow the electrons to saturate in passing through the laser. We emphasize here that the saturation mechanisms are different in the low and high gain regimes. This saturation occurs at $A_0^2 \simeq 0.06$ for $G = 4.0$, and $A_0^2 \simeq 500$ for $G = 0.6$. We note that in the high gain case, $G = 4.0$, the value $A_0^2 \simeq 0.06$ cannot be considered of low real intensity. For example, in the previous parameters for the UTFEL where $\rho \simeq 0.0028$, we can see from the definition of A^2 in (1) that a scaled intensity of $A_0^2 \simeq 0.06$ corresponds to a real intensity of $\simeq$ MWcm^{-2}.

The gain at saturation [defined by (6)] as read from Fig. 3 is $\simeq 2.0/0.06 \simeq 33$ for the high gain, and $\simeq 6.0/500 \simeq 0.012$ for the low gain.

The optimum reflectivity (R_{opt}) for maximizing the output intensity can be estimated by substituting for A_0^2 and A_G^2 at saturation into (9). For the high gain $R_{\text{opt}} \simeq 0.06/2.0 = 0.03$, and for the low gain $R_{\text{opt}} \simeq 500/506 \simeq 0.988$.

Information about the efficiency is also available from the figure using (4). If we consider the low and high gain FEL's to have identical number of wiggler periods (N_w), the different values of G are due only to the difference in the value of ρ, and the ratio of the high to low gain efficiencies is

$$\frac{\eta_{\text{HG}}}{\eta_{\text{LG}}} = \frac{G_{\text{HG}} A_{\text{HG}}^2}{G_{\text{LG}} A_{\text{LG}}^2} \simeq \frac{8.0}{3.6} \simeq 2.2.$$

That is, the high gain system is more efficient by a factor 2.2. If the difference between the high and low gain systems is due only to the number of wiggler periods N_w then both systems have identical ρ, and thus from (5), $\eta_{\text{HG}}/\eta_{\text{LG}} = 2.0/6.0 = 1/3$, so that the low gain system has a higher efficiency by a factor of 3. This perhaps initially surprising result is due to the different saturation mechanisms between the low and high gain systems.

Similarly, by using (4) the ratio of high to low gain real intensities is $\simeq 656$ if the difference in G is due to n_e only, and $\simeq 1/3$, (necessarily from the above ratio for the efficiency), if due to difference in the N_w only.

We now use the tabular method described in the previous section to follow the scaled output intensity A_{out}^2, for the same values of $G = 0.6$ and $G = 4.0$, as a function of the number of round-trips (n) in the oscillator cavity. Initial intensities of $A_0^2 = 10^{-6}$ were used, and output mirror reflectivities of $R = 0.4$, for the high gain, and $R = 0.988$ for the low gain. The results of the simulations are shown in Fig. 4. The bottom scale refers to the low-gain curve (a), and the top scale to the high gain curve (b).

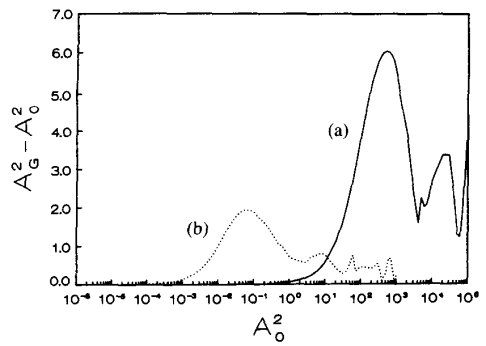

Fig. 3. Difference of output and input scaled intensities ($A_G^2 - A_0^2$) as function of A_0^2 for single-pass amplifier configuration for gain parameters (a) $G = 0.6$ (low gain) and (b) $G = 4.0$ (high gain).

We notice that the estimate of $R \simeq 0.988$ does in fact correspond to the optimum reflectivity for maximum efficiency in the low gain case, as the scaled output intensity rises to the maximum possible of $A_{out}^2 \simeq 6.0$.

This is not the case for the high gain system, however, as the steady-state output is $A_{\text{out}}^2 \simeq 1.0$, approximately half that value that should be available according to Fig. 3. The intensity rises quickly within five round trips to a maximum of $\simeq 1.2$ then decreases to the steady-state value of $\simeq 1.0$. The intensity in the steady state at the beginning of the wiggler will then be $A_0^2 \simeq R \cdot 1.0 = 0.4$, and as seen from Fig. 3 this means that the electrons–radiation will have saturated before the end of the wiggler and entered the synchrotron oscillatory phase of evolution. Clearly then a lower reflectivity mirror is required to obtain maximum efficiency.

In order to investigate further the effect of the output mirror reflectivity, many simulations were performed through the complete range of R, $0 < R < 1$, for three values of G (0.6, 1.5 and 4.0). The simulations were run (with $A_0 = 10^{-6}$ for the first-round trip) until a stable steady output intensity was attained. These scaled steady-state output intensities are plotted as a function of the output mirror reflectivity R in Fig. 5.

For the case of the low gain ($G = 0.6$) it is seen that only a narrow range of R takes the laser above threshold. The cutoff is at $R \simeq 0.94$, implying a small-signal gain of $\simeq 0.06$, which has been confirmed directly from the linear theory. Maximum output intensity is at $A_{\text{out}}^2 \simeq 6.0$, as is expected from previous discussions.

For the case of the high gain ($G = 4.0$), the maximum efficiency is for $R \simeq 0.03$, as expected. Below this value of R, the output intensity drops rapidly to that value obtained for a single-pass device with initial intensity $A_0^2 = 10^{-6}$. We see then that in a high gain system which cannot saturate from noise (or a low intensity input signal) in a

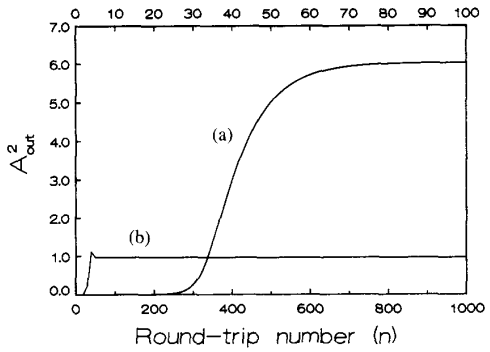

Fig. 4. Scaled output intensities A^2_{out} from FEL oscillator as function of the round trip number (n), with (a) $G = 0.6$, $R = 0.988$ (bottom scale), and (b) $G = 4.0$, $R = 0.4$ (top scale).

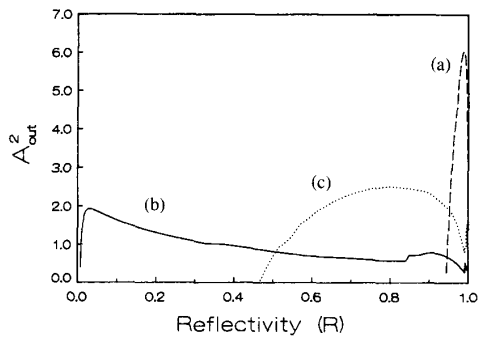

Fig. 5. Steady-state scaled output intensities A^2_{out} from FEL oscillator as function of output mirror reflectivity R for (a) $G = 0.6$, (b) $G = 4.0$, and (c) $G = 1.5$.

single-pass configuration, by using a low Q cavity the system can quickly reach a saturated output intensity.

We note that for values of R greater than the value for maximum efficiency the electrons–radiation will have entered the synchrotron–oscillatory phase of evolution before exiting the wiggler. Conversely, for values of R below the optimum the electrons–radiation will not yet have saturated.

In Fig. 6, we plot the maximized ($R = R_{opt}$) steady-state output intensity times the gain parameter G as a function of G. This function is proportional to the maximum efficiency η_{max} available from an FEL oscillator for a given G:

$$GA^2_{out} = 4\pi\rho N_w A^2_{out} = 4\pi N_w \eta_{max} \qquad (10)$$

where we have used (5).

In the low gain $G < 1$, $\eta_{max} \simeq 3.6/4\pi N_w$ (consistent with the inequality $\eta_{max} < 1/2N_w$ for low gain systems [1]). From (4) and (5) we also see that as $N_w\eta_{max}$ is a constant that the real intensity scales as $|E|^2 \propto n_e$.

In the high gain $G > 1$, $N_w\eta_{max}$ increases nonlinearly as a function of G for $1 \cdot 0 < G < 4.0$. The maximum gradient in this region is $d(N_w\eta_{max})/dG \simeq 2.0$ between $G \simeq 3.0$ and 4.0. For $G > 4.0$ there is a quasi-linear increase in $N_w\eta_{max}$ with gradient $\simeq 1.25$ to 1.3. This rather

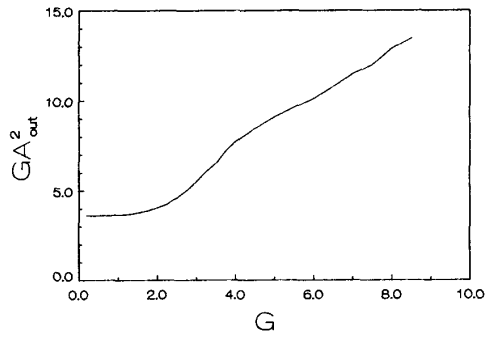

Fig. 6. Steady-state scaled output intensity A^2_{out} times gain parameter G, for optimized mirror reflectivity R_{opt} as function of G. (Note $GA^2_{out} = 4\pi N_w \eta$.)

complicated behavior is thought to arise due to the choice of the optimized detuning parameter δ_{opt} for the initial conditions of the electrons. If a detuning of $\delta = 0$ were chosen for all values of $G > 1$ (clearly not optimized for maximum gain—see Fig. 1), $N_w\eta$ would not rise as quickly from $G = 1$ as in Fig. 6, and should tend asymptotically to a linearly increasing value such that $GA^2_{out} \simeq 1.4G$, giving a gradient of $\simeq 1.4$ (the value 1.4 here being the approximate value of the saturated scaled intensity A^2_{sat} in the limit $G >> 1$ see [2], [8]). We could then expect that if the curve in Fig. 3 were extrapolated to larger values of G (and assuming that the radiation–electrons did not saturate in the first pass through the wiggler) then it would tend to the same asymptote with gradient $\simeq 1.4$.

The general macroscopic behavior, however, is of a linear increase in $N_w\eta_{max}$ from $G \simeq 2.0$. This scaling of $\eta_{max} \propto G$ implies the real intensity scales as $|E|^2 \propto n_e^{4/3}$ for identical wigglers. It is for this reason that we say the region between $G \simeq 1.0$ and 2.0 is the transition region between the low and high gain regimes.

Finally, in Fig. 7 we plot the optimized output mirror reflectivity R_{opt} corresponding to the maximum efficiencies of Fig. 6.

Conclusion

The results presented here are not intended to predict with great accuracy real quantities, such as the output intensity, in any given FEL experiment. The initial assumptions of a plane-mirror cavity and the continuous 1-D electron beam assure this. The results do however show the effects and scaling involved in passing from the low into the high gain in an FEL oscillator.

This is of particular interest in the University of Twente and the Los Alamos experiments outlined, as the new generation of photocathode injectors may make available the current to take these experiments from the low–high gain threshold, into the region where high gain evolution dominates.

One of the major restrictions of the model used here is the assumption of a continuous electron beam. The tabular method of modeling the radiation evolution cannot be

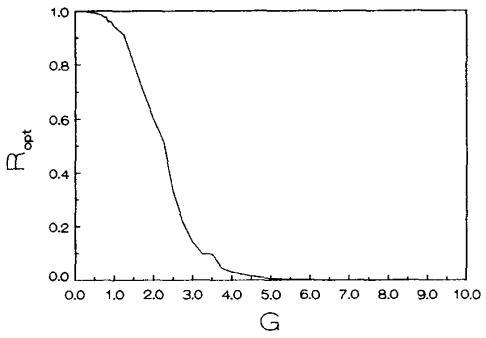

Fig. 7. Optimized output mirror reflectivity R_{opt} as function of gain parameter G.

modified easily to model radiation emitted from electron pulses. This is an area which is well worth investigation in light of recent work on super-radiant pulses in FEL amplifiers [9], and is currently underway.

The tapering of the wiggler to improve efficiency has also not been considered. It is thought, however, that the radiation evolution in steady-state tapered wiggler FEL's should in principal be modeled effectively by using the tabular method.

Acknowledgment

The author would like to thank G. J. Ernst, E. H. Haselhoff, P. J. M. Van Der Slot, and W. J. Witteman of the University of Twente, and also R. Bonifacio of the University of Milano for helpful suggestions and discussions relating to this work.

References

[1] T. C. Marshall, *Free Electron Lasers*. New York: Macmillan, 1985.
[2] R. Bonifacio, C. Pellegrini, and L. M. Narducci, "Collective instabilities and high gain regime in a free electron laser," *Opt. Commun.*, vol. 50, no. 6, pp. 373–378, July 1984.
[3] W. B. Colson, "One body electron dynamics in a free electron laser," *Phys. Lett. A*, vol. 64, pp. 190–192, 1977.
[4] R. L. Sheffield, E. R. Gray, and J. S. Fraser, "The Los Alamos photoinjector program," *Nucl. Instrum. Meth.*, vol. A272, pp. 222–226, 1988.
[5] B. E. Newnam, R. W. Warren, R. L. Sheffield, W. E. Stern, M. T. Lynch, J. S. Fraser, J. C. Goldstein, J. E. Sollid, T. A. Swann, J. M. Watson, and C. A. Brau, "Optical performance of the Los Alamos free electron laser," *IEEE J. Quantum Electron.*, vol. QE-21, pp. 867–881, July 1985.
[6] W E. Stein, R. W. Warren, J. G. Winston, J. S. Fraser, and L. M. Young, "The accelerator for the Los Alamos free electron laser-IV," *IEEE J. Quantum Electron.*, QE-21, pp. 889–894, July 1985.
[7] G. J. Ernst *et al.*, "Proposal for a race-track microtron with a high peak current," in *Proc. 10th Int. FEL Conf.*, Jerusalem, Israel, 1988, to be published.
[8] R. Bonifacio, F. Casagrande, and L. De Salvo Souza, "Generalized gain spread relation and optical guiding in high gain free electron laser amplifiers," *Opt. Commun.*, vol. 58, no. 4, pp. 259–264, June 1986.
[9] R. Bonifacio and B. W. J. McNeil, "Slippage and superradiance in the high gain FEL," *Nucl. Instrum. Meth.*, vol. A272, pp. 280–288, 1988.
[10] B. W. J. McNeil and W. J. Firth, "Gain in planar wiggler free electron lasers," *Nucl. Instrum. Meth.*, vol. A259, pp. 240–244, 1987.

B. W. J. McNeil, photograph and biography not available at the time of publication.